DOI: 10.1002/chem.201301379

Salimabromide: Unexpected Chemistry from the Obligate Marine Myxobacterium *Enhygromxya salina*

Stephan Felder,[a] Sandra Dreisigacker,[b] Stefan Kehraus,[a] Edith Neu,[a] Gabriele Bierbaum,[c] Patrick R. Wright,[a] Dirk Menche,[b] Till F. Schäberle,[a] and Gabriele M. König*[a]

Abstract: Marine myxobacteria (*Enhygromyxa*, *Plesiocystis*, *Pseudoenhygromyxa*, *Haliangium*) are phylogenetically distant from their terrestrial counterparts. Salimabromide is the first natural product from the *Plesiocystis*/*Enhygromyxa* clade of obligatory marine myxobacteria. Salimabromide has a new tetracyclic carbon skeleton, comprising a brominated benzene ring, a furano lactone residue, and a cyclohexane ring, bridged by a seven-membered cyclic moiety. The absolute configuration was deduced from experimental and calculated CD data. Salimabromide revealed antibiotic activity towards *Arthrobacter cristallopoietes.*

Keywords: enhygromyxa · myxobacteria · natural products · NMR spectroscopy · polyketides

Introduction

Marine myxobacteria are hardly investigated. The only known metabolite of obligate marine origin is haliangicin from *Haliangium ochraceum* (Figure 1).[1] To a very minor extent, secondary metabolites of slightly halophilic myxobacteria, such as the miuraenamides, have been described.[2] In an earlier study, we were successful in obtaining the multidrug reversal agent phenylnannolone A from a strain of *Nannocystis exedens* from the intertidal area.[3] In contrast, terrestrial myxobacteria are known for their ability to produce a wide range of secondary metabolites with a remarkable abundance of new skeletons,[4] for example, macrodilactones (such as leupyrrin A),[5] bithiazoles (such as cystothiazole A),[6] spiroketal moieties (as was found in spirangien A),[7] macrolactones (such as etnangien),[8] lipopeptides (represented by myxochromide A),[9] and α-pyrones, exemplified by corallopyronin A.[10]

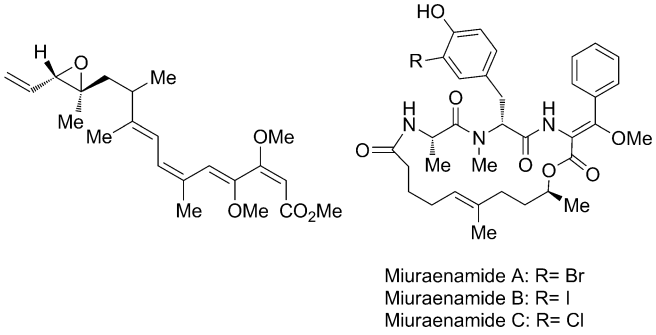

Figure 1. Structure of haliangicin, the only known myxobacterial metabolite from an obligatory marine bacterium and of miuraenamide A-C from the slightly halophilic *Paraliomyxa miuraensis.*

The focus of the current study is on unusual, hitherto not at all researched bacterial taxa, which are a promising source for structural diversity.[11,12] We were successful in isolating an obligatory marine myxobacterium from a mud sample from the coast of the island Prerow (Germany). 16S rDNA analysis revealed that this bacterium is *Enhygromyxa salina*, a species closely related to microorganisms hitherto termed as "unculturable".[13] Due to a persistent antibiotic activity towards gram-positive microorganisms, this strain was chosen for detailed investigation.

Large-scale cultivation made it possible to isolate the first secondary metabolite, that is, **1**, from this marine myxobacterium. The compound is only produced in minute amounts of 8 $\mu g L^{-1}$. Salimabromide (**1**) has a new carbon skeleton, and the core structure revealed no resemblance to any known natural or synthetic compound. If considered in conjunction with the results from phylogenetic analysis and first data from a draft genome of strain SWB007 of *E. salina*, our finding reflects that marine myxobacteria are phylogeneti-

[a] S. Felder, Dr. S. Kehraus, E. Neu, P. R. Wright, Dr. T. F. Schäberle, Prof. Dr. G. M. König
Institute for Pharmaceutical Biology
University of Bonn
Nussallee 6, 53115 Bonn (Germany)
Fax: (+49) 228-733250
E-mail: g.koenig@uni-bonn.de

[b] Dr. S. Dreisigacker, Prof. Dr. D. Menche
Kekulé-Institute for Organic Chemistry and Biochemistry
University of Bonn
Gerhard-Domagk-Strasse 1, 53121 Bonn (Germany)

[c] Prof. Dr. G. Bierbaum
Institute of Medical Microbiology, Immunology and Parasitology
University of Bonn
Sigmund-Freud-Strasse 25, 53105 Bonn (Germany)

Supporting information for this article is available on the WWW under http://dx.doi.org/10.1002/chem.201301379.

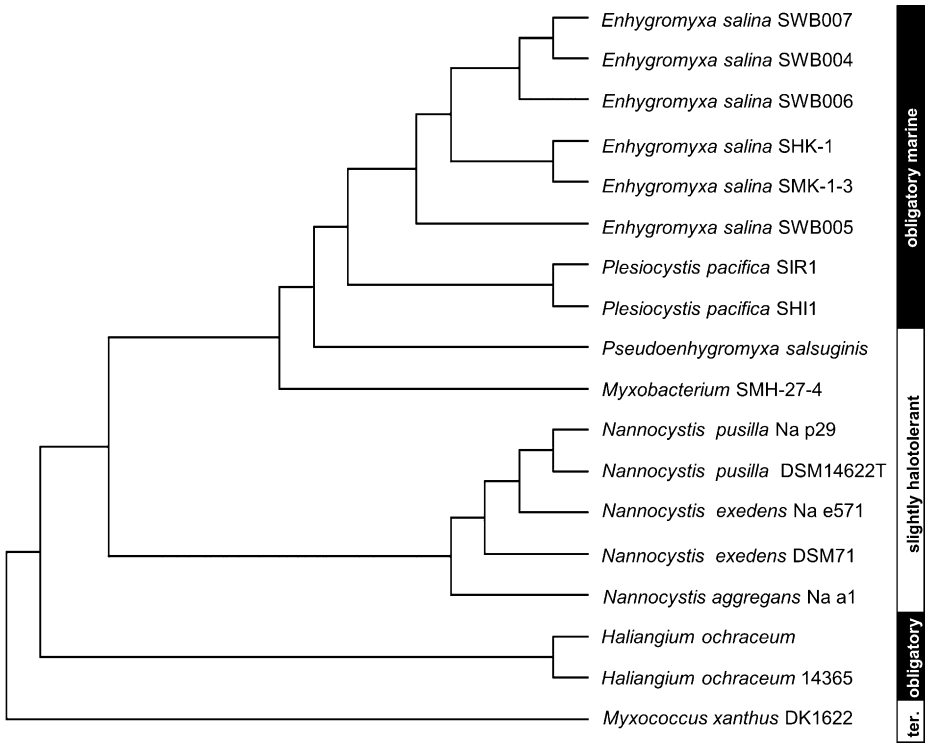

Figure 2. Phylogeny of marine and halophilic myxobacteria (*Nannocystineae*) based on 16S rDNA. *Enhygromyxa salina* SWB007 is the herein investigated strain; the tree is rooted with the terrestrial myxobacterium *Myxococcus xanthus* DK1622 (ter = terrestrial).

cally quite distinct from other myxobacteria, which is also mirrored in their biosynthetic abilities (Figure 2).

Results

Phylogeny of marine myxobacteria: Recent findings evidence that myxobacteria, which were originally described as merely occurring in terrestrial environments, such as soil, are also present in numerous marine sediments.[13–15] However, their isolation and cultivation is in most cases not possible to date, and thus the corresponding secondary metabolome is completely unknown. Until now, merely a few isolates could be cultured under laboratory conditions, and of these, only *Enhygromyxa*, *Haliangium*, and *Plesiocystis* represent obligatory marine genera (Figure 2).

In contrast to this, bacteria of the *Nannocystis* clade and of the newly suggested genus *Pseudoenhygromyxa*,[16] both mostly isolated from brackish water or intertidal areas, are also able to grow without salt, but tolerated NaCl concentrations lower than those of sea water.

The *Haliangiaceae*, showing higher similarity to the terrestrial myxobacteria based on 16S rDNA analysis, branched earlier, and tolerated the highest sea-salt concentrations. Herein, we describe the first natural product isolated from the *Plesiocystis*/*Enhygromyxa* clade (suborder *Nannocystineae*) of obligatory marine myxobacteria.

Isolation and structure elucidation: The bacterium was cultivated in marine media under addition of an adsorber resin. After extraction of the resin and the bacterial pellet with acetone, the resulting extract was fractionated by liquid/liquid partitioning, and the lipophilic extract was separated by using normal-phase-vacuum liquid chromatography and solid-phase extraction. Finally, reversed-phase (RP) HPLC separations gave salimabromide (**1**) (Figure 3).

The molecular formula of salimabromide was determined to be $C_{20}H_{20}Br_2O_3$ by using mass spectral (HRMS (EI): m/z 465.9779) and NMR data analyses, and implies ten double-bond equivalents. The IR spectrum revealed characteristic absorption bands for a lactone

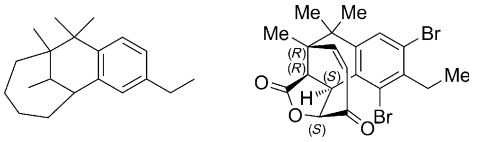

1

Figure 3. New tricyclic carbon skeleton of **1** and structure of salimabromide.

functionality ($\tilde{\nu} = 1780\ cm^{-1}$) and a ketone ($\tilde{\nu} = 1685\ cm^{-1}$).[17] The aromatic nature of salimabromide was evident from an UV maximum at $\lambda = 275$ nm. The ^1H NMR spectrum confirmed the presence of an aromatic moiety (6-H, $\delta = 7.65$ ppm, s), which according to the singlet resonance of 6-H had to be penta-substituted (Table 1). Furthermore, the ^1H NMR spectrum displayed two resonances for protons associated with a carbon–carbon double bond (3-H, $\delta =$ 6.35; 9-H, 5.70 ppm), a proton adjacent to oxygen (11-H, $\delta = 5.65$ ppm, d) and four methyl groups (17-H_3, $\delta = 1.25$, s; 18-H_3, 1.52, s; 19-H_3, 1.61, s; 20-H_3, 1.17 ppm, t). Of the latter, three (17-H_3 to 19-H_3) are located on quaternary carbons, whereas 20-H_3, giving rise to a triplet resonance, had to be next to a methylene group (16-H_2, $\delta = 3.09$ ppm, q). In the ^{13}C NMR spectrum resonances for 20 carbon atoms were present, which can be grouped into nine quaternary carbons, six methine, a methylene and four methyl groups, as was deduced from a distortionless enhancement by polarization transfer (DEPT) measurement. Of the nine quater-

Table 1. 1D and 2D NMR spectroscopic data (500 MHz, [D_4]MeOH) of salimabromide (w = weak signal).

Position	δ_C, mult. [ppm]	δ_H (J in Hz) [ppm]	COSY [ppm]	HMBC [ppm]
1	197.7, C			
2	177.9, C			
3	149.8, CH	6.35, d (13.1)	9, 13(w)	1, 13, 19
4	147.6, C			
5	142.7, C			
6	131.5, CH	7.65, s		5, 7, 10, 14
7	130.1, C			
8	128.1, C			
9	126.5, CH	5.70, d (13.1)	3	3(w), 11, 12
10	125.7, C			
11	83.5, CH	5.65, d (8.5)	15	1(w), 2, 9(w), 13(w), 15
12	45.8, C			
13	45.2, CH	3.38, d (8.5)	3(w), 15	2, 3, 11, 12, 15, 19(w)
14	44.7, C			
15	42.6, CH	4.44, t (8.5)	11, 13	1, 4(w), 7, 8, 11, 13
16	31.9, CH_2	3.09, q (7.6)	20	5, 8, 10, 20
17	29.1, CH_3	1.25, s		4, 12, 14, 18
18	22.5, CH_3	1.52, s		4, 12, 14, 17
19	21.8, CH_3	1.61, s		3, 12, 13, 14
20	12.7, CH_3	1.17, t (7.6)	16	5, 16

nary carbons, five were attributed to the aromatic ring (weak signals at $\delta = 147.6$ (C4), 142.7 ppm (C5), 130.1 ppm (C7), 128.1 (C8), and 125.7 ppm (C10)). For the hydrogen-substituted aromatic carbon, the ^{13}C NMR spectrum displayed an intense resonance signal at $\delta = 131.5$ ppm (C6). Due to their characteristic ^{13}C NMR chemical shifts (C3, $\delta =$ 149.8; C9, 126.5 ppm), two sp^2-hybridized carbon atoms were identified as associated with the olefinic partial structure. ^{13}C NMR resonances for the two quaternary carbons C1 ($\delta = 197.7$ ppm) and C2 ($\delta = 177.9$ ppm) indicated them to be involved in an ester and a carbonyl functional group, respectively, whereas the sp^3-hybridized carbon resonating at $\delta = 83.5$ ppm (C11) had to be attached to an oxygen atom. This left two quaternary, sp^3-hybridized carbon atoms to be accounted for (C12, $\delta = 45.8$; C14, 44.7 ppm), as well as two further sp^3-hybridized carbon atoms with resonance signals discernible at $\delta = 45.2$ (C13) and 42.6 ppm (C15).

2D-NMR spectra (^1H–^1H correlation spectroscopy (COSY), ^1H–^{13}C heteronuclear single-quantum coherence (HSQC), and ^1H–^{13}C heteronuclear multiple-bond correlation (HMBC)) revealed homo- and heteronuclear couplings and thus enabled the structure of salimabromide to be delineated. The molecule can be divided into two main structural elements, that is, A and B (Figure 4). Partial structure A was identified to be the penta-substituted phenyl ring, clearly characterized by HMBC correlations. Thus, 6-H showed correlations to the quaternary carbons C5, C7, and C10 completing the aromatic ring. A ^1H–^1H COSY spectrum indicated an ethyl moiety (16-H_2, $J =$ 7.6 and 20-H_3, 7.6 Hz), which had to be connected to carbon C5 due to HMBC correlations from 16-H_2 to C5, C8 and C10, and of 20-H to C5.

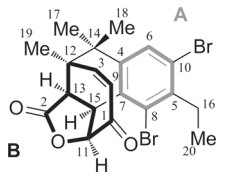

Figure 4. Partial structures A and B of salimabromide.

The ^1H–^1H COSY spectrum depicted two isolated spin systems for partial structure B. The first one comprised the protons of a double bond (3-H, $\delta = 6.35$ ppm, $J = 13.1$ Hz and 9-H, 5.70 ppm, 13.1 Hz). A second ^1H–^1H spin system was found to involve 11-H ($\delta = 5.65$ ppm, $J = 8.5$ Hz, d), 13-H ($\delta = 3.38$ ppm, $J = 8.5$ Hz, d), and 15-H ($\delta = 4.44$ ppm, $J =$ 8.5 Hz, t), in which 15-H had to be located between 11-H and 13-H due to the triplet resonance observed for this proton. HMBC correlations of these three methine protons established further connectivities within substructure B. Thus, the connection of C11 to C2 though oxygen, and of C13 to C2 was indicated by heteronuclear couplings of 11-H and 13-H to C2. 11-H also showed HMBC cross correlations to C1, whereas 13-H had heteronuclear couplings to C12 and C3, which established the seven-membered ring and completed fragment B.

The connection of partial structures A and B though a C15/C7 bond on one side was evident from an HMBC correlation from 15-H to C7. Methyl groups CH_3-17 and CH_3-18 both had to be linked to the same carbon, that is, C14 based on their identical heteronuclear couplings. On this upper side of the molecule, C14 had to be linked to the aromatic carbon C4 due to an HMBC correlation of 6-H to C14. At this stage only, one further bond had to be established for the basic structure of salimabromide, which was deduced to be located between C12 and C14, easily discernible from the HMBC correlation of 19-H_3 to C14. According to the molecular formula, two bromine atoms were to be positioned in the molecule. By deduction, they had to be linked to the aromatic carbon atoms C8 and C10.

The structure of salimabromide was supported by additional NMR spectroscopy data. Thus, 3-H showed a weak ^1H-^1H *W*-coupling to 13-H, which is clearly reflected in the proposed structure. The position of the methyl groups CH_3-17/18 and CH_3-19 was also obvious from NOE correlations, that is, 18-H_3 was close in space to 6-H, 17-H_3, and 19-H_3. Also indicative for the structure of salimabromide were NOEs from 19-H_3 to 3-H and 13-H, showing the proximity of all of these centers within the molecule.

Proton-coupling constants and NOEs also allowed conclusions on the relative configuration of the compound (Figure 5). The *Z* configuration of the $\Delta^{3,9}$ double bond was proven by NOE correlations between 3-H and 9-H, and was also supported by a $J_{3/9}$ ^1H–^1H coupling constant of 13.1 Hz, which is typical for a *cis*-configurated double bond in seven-membered rings.[18] Diagnostic NOEs could be observed from 15-H to 13-H and to 11-H, from 19-H_3 to 13-H and to 17-H_3, proving all of these protons to be on the α-side of the molecule. Concluding from this, the C1/9/3 bridge had to be on the upper side of the molecule, which was also evidenced by NOEs from 3-H to the δ-positioned 18-H_3. Coupling constants of 11-H, 13-H, and 15-H are in good agreement with the dihedral angles extracted from the model according to the Karplus Equation (Figure 5).[19] Taking all these data to-

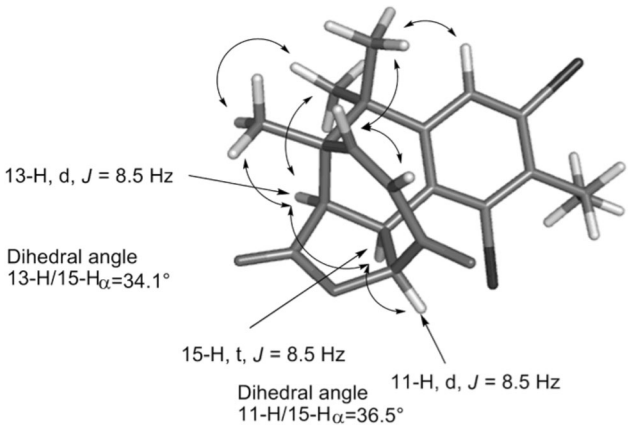

Figure 5. NOE correlations of salimabromide that reveal together with ^{1}H–^{1}H coupling constants the relative configuration (3D-structure of (**1**) derived from DFT optimization at B3LYP/6-31G(d) level of theory).

gether, the relative configuration of salimabromide was established.

The absolute configuration at the chiral centers C11, C12, C13, and C15 was deduced by analysis of circular-dichroism (CD) spectroscopic data. Considering the UV spectrum of salimabromide, only weak Cotton effects in the range of $\lambda =$ 200–220 nm were expected. Indeed, the experimental data showed a positive Cotton effect at $\lambda = 209$ nm ($\Delta\varepsilon + 0.65$) and negative one at $\lambda = 216$ nm ($\Delta\varepsilon - 1.12$).

The CD spectra for both possible enantiomers were calculated (see Computational Details in the Experimental Section) and compared with the experimental data. This revealed that the natural product has the 11*S*, 12*R*, 13*R*, and 15*S* configuration (Figure 6).

Antimicrobial testing: Salimabromide was tested against a broad spectrum of microorganisms and revealed a moderate antibiotic activity against *Arthrobacter cristallopoedes* with an MIC value of 16 $\mu g\,mL^{-1}$.

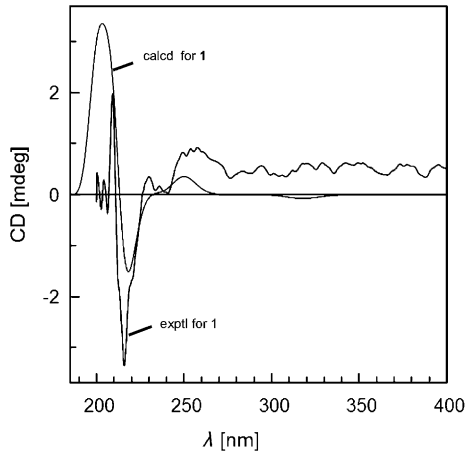

Figure 6. Stereochemical assignment of the absolute configuration of salimabromide (**1**). Comparison of the calculated CD spectrum for the 11*S*, 12*R*, 13*R*, and 15*S* isomer of **1** with the experimental CD spectrum.

Discussion

Marine myxobacteria may be divided into two groups, that is, the herein targeted *Nannocystineae*, thought to represent a group, which adapted from a terrestrial life style to the marine environment, and the recently reported exclusively "marine myxobacterial cluster" (MMC) only detected based on their genetic fingerprint with no cultured representatives.[14] The fact that only one secondary metabolite, that is, haliangicin of strict marine myxobacterial origin is known,[1] reflects the difficulty in the isolation and cultivation of these unique bacteria (Figure 1). Haliangicin has as a prominent structural feature a β-methoxyacrylate substructure, being the pharmacophor for its antifungal activity, a property which it has in common with metabolites from terrestrial myxobacteria, for example, cyrmenins, myxothiazol, and cystothiazole.[6,20,21]

In contrast, salimabromide (**1**), the first secondary metabolite from the genus *Enhygromyxa*, revealed a new carbon skeleton with extraordinary features (Figure 3). The tricyclic core structure is composed of annelated benzene, cyclohexane, and cycloheptane rings. The furano lactone moiety adds a rigid element to the structure, greatly diminishing the conformational flexibility of the compound. Unusual substitutions are the ethyl side chain on the aromatic ring, which occurs rarely in natural products, however, some prominent bioactive compounds, such as kirromycin[22] and spiramycin,[23] are also ethyl substituted.

Furthermore, the substitution with bromine emphasizes the marine origin of this compound.[24] In general, halogenated myxobacterial metabolites are rare, the only examples being the chlorinated chlorotonil, chondrochloren, maracen A, pedein A, pyrrolnitrin (also present in *Pseudomonas*), and hyaladione. However, in this context, again the chlorinated, brominated, or even iodine-substituted miuraenamides have to be mentioned, derived from a myxobacterium from a soil sample next to the sea shore.[2] The latter are the only brominated myxobacterial compounds.

The chemical nature of salimabromide suggests that it is in principle the product of a polyketide synthase (PKS) and one or more halogenases. Most of the identified gene clusters of myxobacteria were elucidated to be PKS/NRPS hybrid systems, whereas PKS on their own are the exception. Thus, of 33 myxobacterial gene clusters described, only seven were defined as PKS, that is, PKS I and II systems.[25] Whole genome sequencing of the GC-rich *E. salina* SWB 007 was done with the goal to obtain first insights into the biosynthesis of salimabromide. Bioinformatic analysis of the obtained sequences revealed the presence of an open reading frame for a halogenase-encoding gene (Figure S10 in the Supporting Information). This halogenase gene was adjacent to sequences for a PKS III system. Type III PKSs are iteratively working multifunctional enzymes, and have for a long time only been known to occur in plants, that is, chalcon/stilben synthases.[26] To date, it is clear however, that they are also found in bacteria, even though they are much less understood than PKS types I and II.

Further studies will address the biosynthesis of this intriguing molecule on the genetic and biochemical level. Especially the unusual rearrangement reactions within the polyketide core will be most fascinating. Upon chemical synthesis of the molecule, a more detailed pharmacological evaluation will be possible.

Conclusion

Salimabromide, isolated from the marine myxobacterium *Enhygromyxa salina*, represents a polyketide with a new tetracyclic carbon skeleton, comprising a brominated benzene ring, a furano lactone residue, and a cyclohexane ring, bridged by a seven-membered cyclic moiety. This study illustrates that marine myxobacteria are phylogenetically, and concerning their secondary metabolome very distinct from their terrestrial counterparts.

Experimental Section

General procedures: UV and IR spectra were recorded with Perkin–Elmer Lambda 40 and Perkin–Elmer Spectrum BX instruments, respectively. The CD spectroscopic measurement was conducted at a Jasco J-810 spectropolarimeter. NMR spectra were recorded at a 500 MHz Bruker Avance 500 DRX spectrometer with [D_4]MeOH as solvent and internal standard. Spectra were referenced to residual solvent signals with resonances at $\delta_{H/C}=3.35/49.00$ ppm. High-performance liquid chromatography was performed on a Waters HPLC system equipped with an in-line degasser AF, 600 controller, 717 plus autosampler, and a 996 photodiode-array detector.

Isolation and taxonomy of the bacterial strain: The marine myxobacterial strain (no. SWB007, strain collection of the Institute for Pharmaceutical Biology, Bonn) was isolated from marine sediments of the coast of Germany, Prerow. The samples were placed on an *E. coli* spot on a water cyclohexamide (WCX) agar plate. After observation of lysis zones, samples were transferred to artificial seawater (VY/4) agar plates and purified throughout several passages until an axenic culture was obtained. The bacterial culture showed characteristic multicellular behavior, such as gliding motility and fruiting body formation, typical for myxobacteria. 16S rDNA analysis revealed that this isolate is *Enhygromyxa salina*. Stock cultures of the strain are kept at −80 °C.

Cultivation and isolation procedure: Cultivation was performed repeatedly in Erlenmeyer flasks (64 flasks, each having a volume of 5 L), each containing artificial seawater medium (1 L; ASW VY/4, trace-elements solution, vitamin B_{12}, 25 mL L^{-1} 10% yeast as nitrogen source), and 30 g L^{-1} of the adsorber resin Sepabeads SP207 (Supelco). The artificial seawater medium consisted of KCl (0.66 g L^{-1}), KBr (0.10 g L^{-1}), NaCl (23.48 g L^{-1}), $MgCl_2 \cdot 6H_2O$ (10.61 g L^{-1}), $CaCl_2 \cdot 2H_2O$ (1.47 g L^{-1}), $SrCl_2 \cdot 6H_2O$ (0.04 g L^{-1}), Na_2SO_4 anhydride (3.92 g L^{-1}), $NaHCO_3$ (0.19 g L^{-1}), and H_3BO_3 (0.03 g L^{-1}).

The Erlenmeyer flasks were each inoculated with two times 100 mL of pre-culture in the same medium. The cultures were shaken on a rotary shaker at 140 rpm for 14 days at 30 °C. Bacterial pellet and adsorber resin were separated from the medium by using a filter (pore size 2) and extracted with acetone (64 × 200 mL). After the organic solvent was removed in vacuo, the residue (13 g) was redissolved in aqueous methanol (60%) and extracted seven times with dichloromethane. Lipophilic crude extract (3.2 g) was obtained and was further separated by vacuum liquid chromatography (VLC) over silica gel (Merck, 63–200 μM, ca. 40 g) by employing petroleum ether, dichloromethane, ethyl acetate, acetone, and methanol as eluents in a stepwise elution process. ^{1}H NMR spectroscopic analysis indicated the ethyl acetate fraction to be of further interest. Solid-phase extraction on reversed-phase material (Bakerbond SPE, C_{18}, 2000 mg) served to prepare the sample for HPLC separation. The fraction of interest was subjected to semipreparative RP-HPLC. The compound was separated by using an isocratic solvent system of methanol/water (75:25) with a Knauer Eurospher C_{18} (250 × 8 mm, 5 μm) column and a flow rate of 1 mL min^{-1}. The pure compound (0.5 mg from 64 L of culture) was obtained after an additional purification step with a Macherey–Nagel 250 × 4.6 mm, 5 μm pentafluorophenyl-propyl (PFP)-modified column and an eluent composed of methanol/water (70:30) with a flow rate of 0.8 mL min^{-1}. The retention time of the salimabromide in this system was 18.7 min.

Salimabromide (1): White amorphous solid (8 μg L^{-1}); $[\alpha]_D^{20}$ + 57.9 deg cm^2 g^{-1} ($c=0.41$ in MeOH); UV (MeOH): λ_{max} (log ε) = 210 (4.6), 275 nm (3.4); CD (MeOH): $\Delta\varepsilon_{209}=+0.65$, $\Delta\varepsilon_{216}=-1.12$ deg cm^2 $dmol^{-1}$; IR (ATR): $\tilde{\nu}_{max}=2921$, 2851, 1780, 1685, 1566, 1441, 1327, 1220, 1162, 1031, 833, 733 cm^{-1}; for ^{1}H and ^{13}C NMR data see Table 1; HRMS (EI): *m/z* calcd for $C_{20}H_{20}Br_2O_3$ (M_w = 468.1850 g mol^{-1}): 465.9779 $[M]^+$; found: 465.9779.

Computational details: ***1) CD spectrum simulation***: Both enantiomers of **1** were built by using the Maestro 9.2 work suite.[27] The structures were preminimized with MMFFs force field (500 iterations) by using Macromodel 9.7 software package (MM).[28] For conformational analysis, the mixed torsion/low-mode sampling algorithm, as implemented in MM, was used. The torsional sampling option was set to extended mode. Default values were used for all other parameters related to the conformational sampling, except that the steps per rotatable bond were set to 10000. The conformational searches were done in aqueous solution with the generalized born/solvent accessible surface (GB/SA) continuum solvation model. The energy minimization was carried out with the Polak–Ribiere conjugate algorithm (PRCG),[29,30] the maximum minimization steps were set to 5000 and the final convergence was set to 0.05 kcal mol^{-1} $Å^{-1}$. For each enantiomer, the conformational search gave just one cluster for the scaffold of the molecule, indicating the rigidity of the structure. The geometry optimization and frequency analysis were performed by using Gaussian 09 software package[31] at B3LYP/6-31G(d) level of theory. The time-dependent DFT excited states calculations were performed with ORCA by using the "chain of spheres" COSX approximation.[32] The single UV and CD spectra were simulated with the hybrid B3LYP functional and Ahlrich's triple zeta Def2-TZVP basis set (*n* states = 20, COSMO = methanol). Before comparison with the experimental CD spectra, a UV correction of −21 nm was accomplished. For Gauss curve generation, UV shifting, comparison with experimental data, and plotting, SpecDis was used.[33]

2) Phylogenetic tree: The phylogenetic tree was constructed by using selected sequences from cultivated bacteria with the respective accession numbers: *Enhygromyxa salina* strain SWB007 (KC818422), *Enhygromyxa salina* strain SWB004 (HM769727), *Enhygromyxa salina* strain SWB006 (HM769729), *Enhygromyxa salina* strain SHK-1 (NR_024807), *Enhygromyxa salina* strain SMK-1-3 (AB097591), *Enhygromyxa salina* strain SWB005 (HM769728), *Plesiocystis pacifica* strain SHI-1 (AB016469), *Pseudoenhygromyxa salsuginis* (AB600195), *Plesiocystis pacifica* strain SIR-1 (NR_024795), *Myxobacterium* SMH-27-4 (AB252740), *Nannocystis pusilla* strain Na p29 (GU207878), *Nannocystis pusilla* type strain DSM 14622T (FR749907), Nannocystis exedens strain Na e571 (AJ233947), *Nannocystis exedens* strain DSM71 (NR_040928), *Nannocystis aggregans* strain Na a1 (AJ233945), *Haliangium ochraceum* (EF108312), *Haliangium ochraceum* DSM 14365 (CP001804), *Myxococcus xanthus* DK 1622 (NC_008095). The tree was built by using the program ClustalW with the standard default settings.[34]

Bioassays: Salimabromide was tested against a broad spectrum of microorganisms, that is, the Gram-positive bacteria *Staphylococcus aureus* SG 511, *Micrococcus luteus* ATCC 4698, *Arthrobacter cristallopoedes* DSM 20117, *Corynebacterium xerosis* VA 167198, the Gram-negative bacterium *Escherichia coli* JM 83, and the fungus *Candida albicans* I 11134. Tests were performed according to reference [13].

Acknowledgements

For the HRMS (EI) measurement, we thank C. Sondag, Department of Chemistry at the University of Bonn. We are grateful to the German Research Foundation (DFG, FOR854) and the German Center for Infection Research (DZIF) for funding this work.

[1] R. Fudou, T. Iizuka, S. Sato, T. Ando, N. Shimba, S. Yamanaka, *J. Antibiot.* **2001**, *54*, 153–156.
[2] M. Ojika, Y. Inukai, Y. Kito, M. Hirata, T. Iizuka, R. Fudou, *Chem. Asian J.* **2008**, *3*, 126–133.
[3] B. Ohlendorf, S. Leyers, A. Krick, S. Kehraus, M. Wiese, G. M. König, *ChemBioChem* **2008**, *9*, 2997–3003.
[4] K. J. Weissman, R. Müller, *Nat. Prod. Rep.* **2010**, *27*, 1276–1295.
[5] H. B. Bode, H. Irschik, S. C. Wenzel, H. Reichenbach, R. Müller, G. Höfle, *J. Nat. Prod.* **2003**, *66*, 1203–1206.
[6] M. Ojika, Y. Suzuki, A. Tsukamoto, Y. Sakagami, R. Fudou, T. Yoshimura, S. Yamanaka, *J. Antibiot.* **1998**, *51*, 275–281.
[7] J. Niggemann, N. Bedorf, U. Flörke, H. Steinmetz, K. Gerth, H. Reichenbach, G. Höfle, *Eur. J. Org. Chem.* **2005**, *23*, 5013–5018.
[8] H. Irschik, D. Schummer, G. Höfle, H. Reichenbach, H. Steinmetz, R. Jansen, *J. Nat. Prod.* **2007**, *70*, 1060–1063.
[9] W. Trowitzsch-Kienast, K. Gerth, V. Wray, H. Reichenbach, G. Höfle, *Liebigs Ann. Chem.* **1993**, *12*, 1233–1237.
[10] Ö. Erol, T. F. Schäberle, A. Schmitz, S. Rachid, C. Gurgui, M. El Omari, F. Lohr, S. Kehraus, J. Piel, R. Müller, G. M. König, *ChemBioChem* **2010**, *11*, 1253–1265.
[11] T. Lincke, S. Behnken, K. Ishida, M. Roth, C. Hertweck, *Angew. Chem.* **2010**, *122*, 2055–2057; *Angew. Chem. Int. Ed.* **2010**, *49*, 2011–2013.
[12] R. H. Feling, G. O. Buchanan, T. J. Mincer, C. A. Kauffman, P. R. Jensen, W. Fenical, *Angew. Chem.* **2003**, *115*, 369–371; *Angew. Chem. Int. Ed.* **2003**, *42*, 355–357.
[13] T. F. Schäberle, E. Goralski, E. Neu, Ö. Erol, G. Hölzl, P. Dörmann, G. Bierbaum, G. M. König, *Mar. Drugs* **2010**, *8*, 2466–2479.
[14] T. Brinkhoff, D. Fischer, J. Vollmers, S. Voget, C. Beardsley, S. Thole, M. Mussmann, B. Kunze, I. Wagner-Döbler, R. Daniel, M. Simon, *ISME J.* **2012**, *6*, 1260–1272.
[15] R. Garcia, K. Gerth, M. Stadler, I. J. Dogma, Jr., R. Müller, *Mol. Phylogenet. Evol.* **2010**, *57*, 878–887.
[16] T. Iizuka, Y. Jojima, A. Hyakawa, S. Fujii, S. Yamanaka, R. Fudou, *Int. J. Syst. Evol. Microbiol.* Epub ahead of print **2012**, DOI:10.1099/ijs.0.040501-0.
[17] E. Pretsch, T. Clerc, J. Seibl, W. Simon in *Spektroskopische Daten zur Strukturaufklärung Organischer Verbindungen*, 4th ed., Springer, Berlin, **2001**.
[18] J. Peng, K. Walsh, V. Weedman, J. D. Bergthold, J. Lynch, K. L. Lieu, I. A. Braude, M. Kelly, M. T. Hamann, *Tetrahedron* **2002**, *58*, 7809–7819.
[19] M. Karplus, *J. Am. Chem. Soc.* **1963**, *85*, 2870–2871.
[20] T. Leibold, F. Sasse, H. Reichenbach, G. Höfle, *Eur. J. Org. Chem.* **2004**, 431–435.
[21] H. Steinmetz, E. Forche, H. Reichenbach, G. Höfle, *Tetrahedron* **2000**, *56*, 1681–1684.
[22] A. Parmeggiani, P. Nissen, *FEBS Lett.* **2006**, *580*, 4576–4581.
[23] I. Brook, *Clin. Pharmacokinet.* **1998**, *34*, 303–310.
[24] K.-H. van Pee, *Arch. Microbiol.* **2001**, *175*, 250–258.
[25] S. C. Wenzel, R. Müller, *Nat. Prod. Rep.* **2009**, *26*, 1385–1407.
[26] C. Hertweck, *Angew. Chem.* **2009**, *121*, 4782–4811; *Angew. Chem. Int. Ed.* **2009**, *48*, 4688–4716.
[27] Maestro, *version 9.2*, Schrödinger, LLC, New York, NY, **2011**.
[28] Macromodel, *version 9.7*, Schrödinger, LLC, New York, **2009**.
[29] E. Polak, G. Ribiere, *Rev. Franc. Inf. Rech. Oper.* **1969**, *16 RI*, 35–43.
[30] R. Klessig, E. Polak, *SIAM J. Control* **1972**, *10*, 524–529.
[31] Gaussian 09, Revision B.01, M. J. Frisch, G. W. Trucks, H. B. Schlegel, G. E. Scuseria, M. A. Robb, J. R. Cheeseman, G. Scalmani, V. Barone, B. Mennucci, G. A. Petersson, H. Nakatsuji, M. Caricato, X. Li, H. P. Hratchian, A. F. Izmaylov, J. Bloino, G. Zheng, J. L. Sonnenberg, M. Hada, M. Ehara, K. Toyota, R. Fukuda, J. Hasegawa, M. Ishida, T. Nakajima, Y. Honda, O. Kitao, H. Nakai, T. Vreven, J. A. Montgomery, Jr., J. E. Peralta, F. Ogliaro, M. Bearpark, J. J. Heyd, E. Brothers, K. N. Kudin, V. N. Staroverov, R. Kobayashi, J. Normand, K. Raghavachari, A. Rendell, J. C. Burant, S. S. Iyengar, J. Tomasi, M. Cossi, N. Rega, J. M. Millam, M. Klene, J. E. Knox, J. B. Cross, V. Bakken, C. Adamo, J. Jaramillo, R. Gomperts, R. E. Stratmann, O. Yazyev, A. J. Austin, R. Cammi, C. Pomelli, J. W. Ochterski, R. L. Martin, K. Morokuma, V. G. Zakrzewski, G. A. Voth, P. Salvador, J. J. Dannenberg, S. Dapprich, A. D. Daniels, Ö. Farkas, J. B. Foresman, J. V. Ortiz, J. Cioslowski, D. J. Fox, Gaussian, Inc., Wallingford CT, **2009**.
[32] F. Neese, ORCA, *Version 2.9.1*, Max-Planck-Institute for Bioinorganic Chemistry, Mühlheim, Germany, **2012**.
[33] T. Bruhn, Y. Hemberger, A. Schaumlöffel, G. Bringmann, *Version 1.60*, University, Würzburg, Germany, **2012**.
[34] J. D. Thompson, T. J. Gibson, D. G. Higgins, *Curr. Protoc. Bioinformatics.* **2002**, Chapter 2, Unit 2.3. DOI: 10.1002/0471250953.bi0203 s00.

Received: April 11, 2013
Published online: May 22, 2013

